Supplementary Materials

Intrinsic physiological properties of layer 2/3 somatosensory cortical neurons in vivo

We recorded a total of 41 cells from layer 2/3 somatosensory cortex (hindpaw region) from 41 mice. Mean RMP for neurons undergoing CSD was -59.55 ± 1.76 mV: this is within the range of what has been reported for layer 2/3 *in vivo*: -60.3 (Chung et al. 2002; layers 2/3-4), −58.6 mV (Mateo et al. 2011; layer 2/3), -60 mV (Ferster and Jagadeesh 1992; layers 1-5), 66.0 (Zhu and Connors 1999; layers 2-5), -50 to -80 mV (Tan et al. 2011; layers 2-4), -65 and -77 mV (Wilent and Contreras 2004; layers 2-6), -78.9 (Kitamura et al. 2008; layer 2/3).

Principal neurons were classified as cells exhibiting regular spiking (RS) or intrinsically bursting (IB) phenotypes (Connors et al. 1982; McCormick et al. 1985; Connors and Gutnick 1990; Nunez et al. 1993; Zhu and Connors 1999; Nowak et al. 2003; Supplementary Fig. 1A). Most of the neurons (20/28; 71%) exhibited regular spiking firing: cells fired a single AP to depolarizing current pulses, with increased firing frequency to increasing current, but frequency was always less than 100 Hz. Spontaneous recordings showed predominantly single APs, though double action potentials were occasionally seen (5% of cells; Supplementary Fig. 1B left). RS cells exhibited broad action potentials: half-width 1.92 ± 0.13 ms. The interspike interval (ISI) histogram for RS neurons was symmetrical, with an refractory period of 5.6 ms (Supplementary Fig. 1C left).

The remainder of principal neurons had an IB phenotype (8/28; 29%). In these cells, bursts were seen at rest (Supplementary Fig. 1B middle) and at

lower current injections (Supplementary Fig. 1A middle); increasing current intensity changed the firing pattern from IB to RS-like firing without a burst (Wang and McCormick 1993; Timofeev et al. 2000). Bursts consisted of more than three action potentials, with firing frequency more than 100 Hz. Half-width of AP's for IB cells was 2.4 ± 0.2 ms. The interspike interval histogram for IB cells showed a skewed distribution with shorter refractory period of 2 ms (Supplementary Fig. 1C middle), which suggested an increased probability of action potential firing for these bursting neurons. We concluded that our normative data from somatosensory cortex pyramidal cells *in vivo* was consistent with RS and IB pyramidal neuron characteristics reported *in vivo* (Nunez et al. 1993; Zhu and Connors 1999; Nowak et al. 2003).

Less frequently we encountered cells with interneuronal characteristics (n = 3 cells, n = 3 animals) from the same recording locations (layer 2/3, hindpaw somatosensory cortex) as principal cells, using blind patch technique. These cells displayed average resting membrane voltage of -64.42 ± 1.07 mV and input resistance of 154.3 ± 2.53. The half-duration of their action potentials was shorter than observed for RS and IB cells, ranging from varied from 1.12 to 1.82 ms, with a mean of 1.56 ± 0.02 ms. Interneurons were able to fire at higher frequencies than excitatory neurons (Supplementary Fig. 1A right) in response to increasing amplitudes of depolarizing current (>100Hz). Spontaneously interneurons were able to fire double or triple APs (Supplementary Fig. 1B right). The refractory period for interneurons was 4.4 ms and displaced toward lower values in comparison to the RS cells (Supplementary Fig. 1C right). Because of the low number of cells, interneurons were not analyzed for the effects of CSD.

To confirm the identity and layer 2/3 location of our recorded cells, we performed additional experiments using two-photon microscopy-guided recordings (Sutter Movable Objective Microscope with 2 Hamamatsu R6357 photomultiplier tubes; Zeiss 5X/0.27NA, 20X/1.0NA and 40X/1.0NA water immersion objectives; Spectra Physics MaiTai Ti:Sapphire laser, pulse width ≈100 fs, excitation 750-950 nm, emission 535/50 nm (green; GCaMP and GFP fluorescence); 617/75 nm (red; Alexa 594 fluorescence)). The patch pipette was visualized by adding the red dye Alexa594 (50 μM) to the internal solution. Anesthesia and experimental setup otherwise identical to Methods.

We used viral delivery of GCaMP5G (Akerboom et al. 2012; AAV2/1.hSynap.GCaMP5G.WPRE.SV40; Penn Vector Core), injected (typically 0.5μL) through a 1mm burrhole in the somatosensory cortex two weeks prior to recording (S1; 2.5 mm lateral to bregma, 200μm depth to trigger layer II/III expression) to allow visualization of all neurons. In these experiments all cells recorded had a RS phenotype (n = 6 cells, 6 animals). Layer 2/3 location was confirmed by distance measured from pia; principal cell anatomy was confirmed by imaging (Figure 2). We used GAD67-GFP (Δneo) animals (n = 4 cells, 4 animals;Tamamaki et al. 2003), expressing green fluorescent protein under the GAD67 promoter, to identify interneurons. Consistent with other reports (Tamamaki et al. 2003; Sohya et al. 2007), there was sparse GFP labeling, as expected for a GABAergic population (Markram et al. 2004). Morphology of the neurons was also consistent with interneurons (Kawabata et al. 2012). All recordings from GFP-expressing cells had an interneuronal electrophysiological phenotype (Margrie et al. 2003; Avermann et al. 2012) (Supplementary Fig. 2).

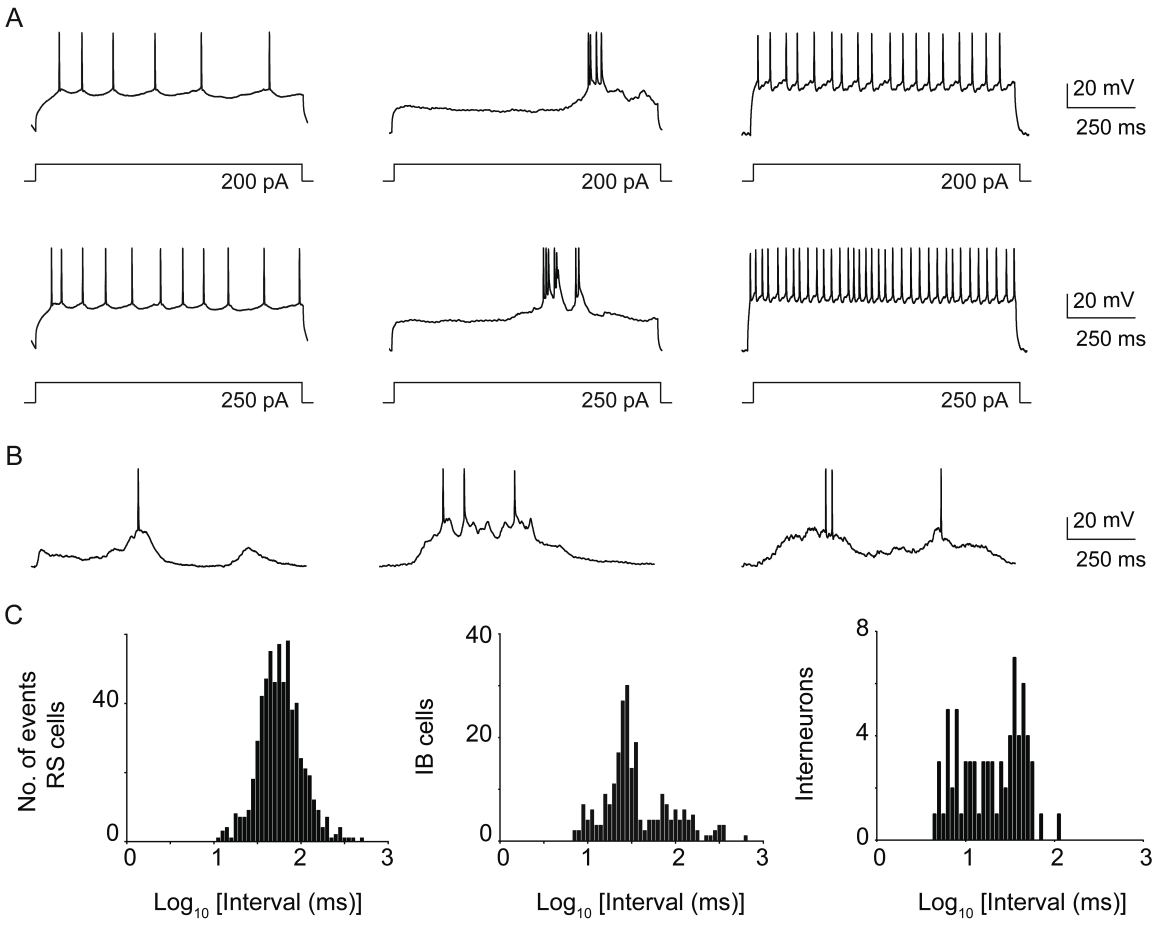

Supplementary Figure 1. *In vivo* whole cell recording in layer 2/3 pyramidal cells and interneurons of sensory cortex: spontaneous and evoked responses of regular-spiking (RS), intrinsically burst-spiking (IB) neurons, and interneurons. (A) Firing profile to depolarizing current pulses of two different current intensities. Action potentials trimmed for clarity. (B) Voltage traces showing spontaneously occurring events. APs trimmed for clarity. (C) Inter-spike interval histograms for RS neurons (left), IB neurons (middle), and interneurons (right) – note the skewed histogram for IB neurons, which reflects burst firing pattern.

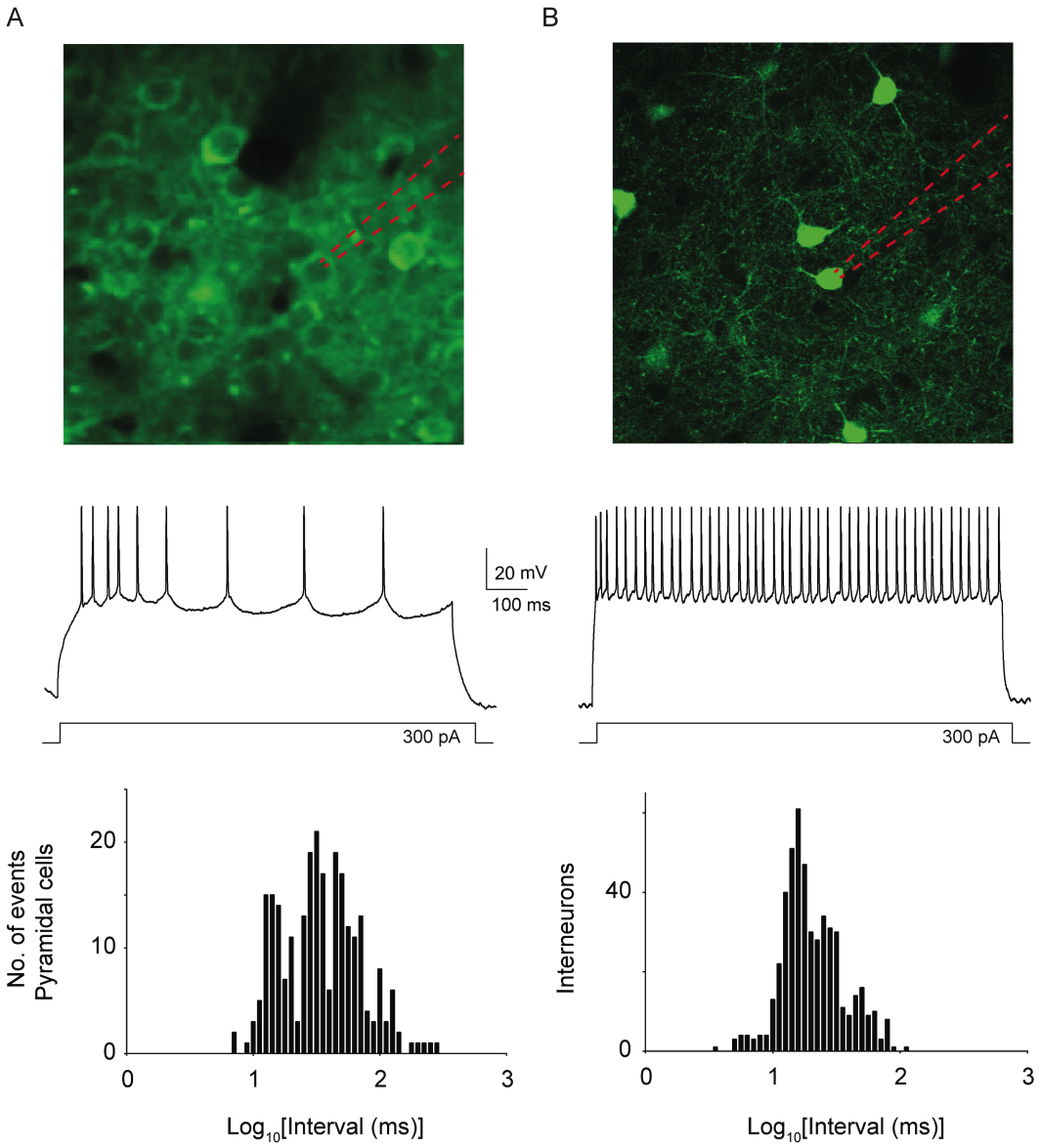

Supplementary Figure 2. A) Image shows neurons expressing GCaMP5 genetically encoded calcium indicator, virally delivered under the synapsin1 promoter, which confers expression in all neurons. Outline of patch pipette in red. Trace shows current clamp recording revealing RS firing pattern on current injection and interspike interval histogram consistent with pyramidal cell identity. All cells recorded with synapsin1-GCaMP5 indicator were RS cells. (B) Two-photon visualization GFP-positive interneuron, imaged from a GAD67-GFP

mouse. Trace shows fast spiking and histogram shows interspike interval histogram consistent with interneuronal characteristics.

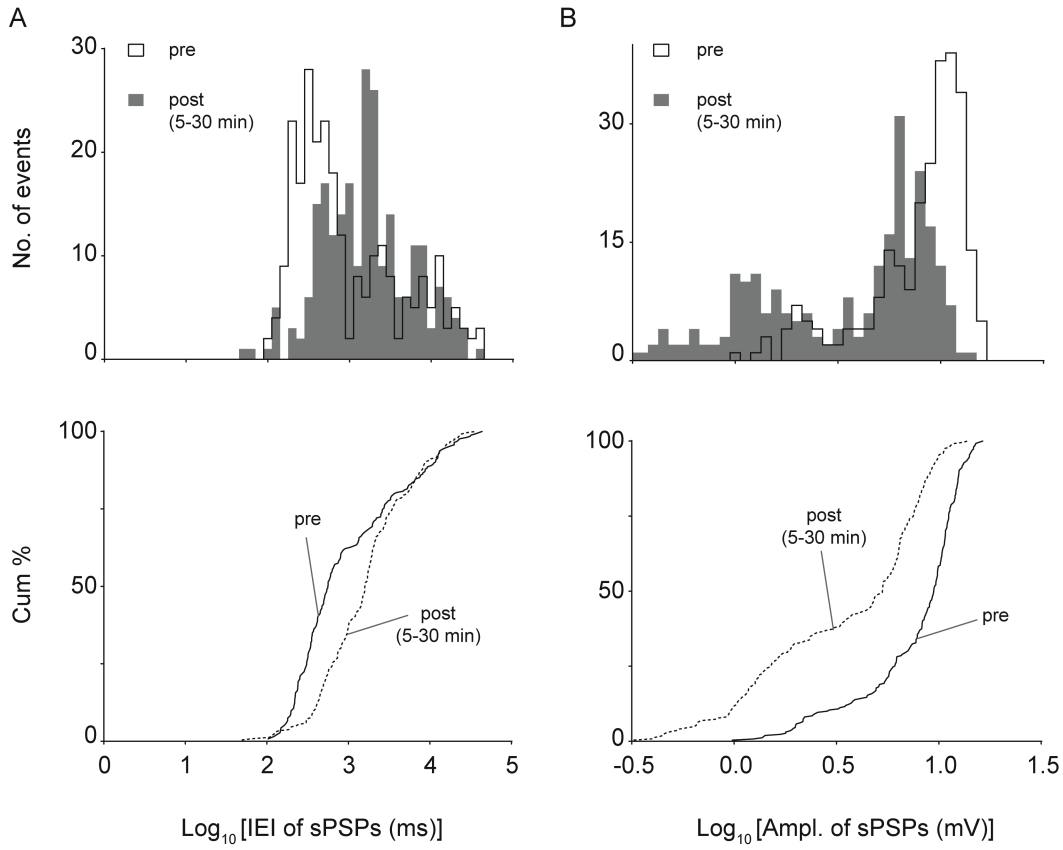

Supplementary Figure 3. Reduced frequency and amplitude of sPSPs from cells patched 5-30 min after CSD *in vivo*. Similar to cells recorded continuously through an CSD event, cells patched 5-30 min *after* CSD show significant reductions in sPSP frequency (A) (KS test, $p = 3.10*10^{-11}$; n = 5 cells, 5 mice) and amplitude ($p = 1.98*10^{-24}$) (B). These results provide evidence that the reductions seen in continuous recordings are unlikely to be due to rundown.

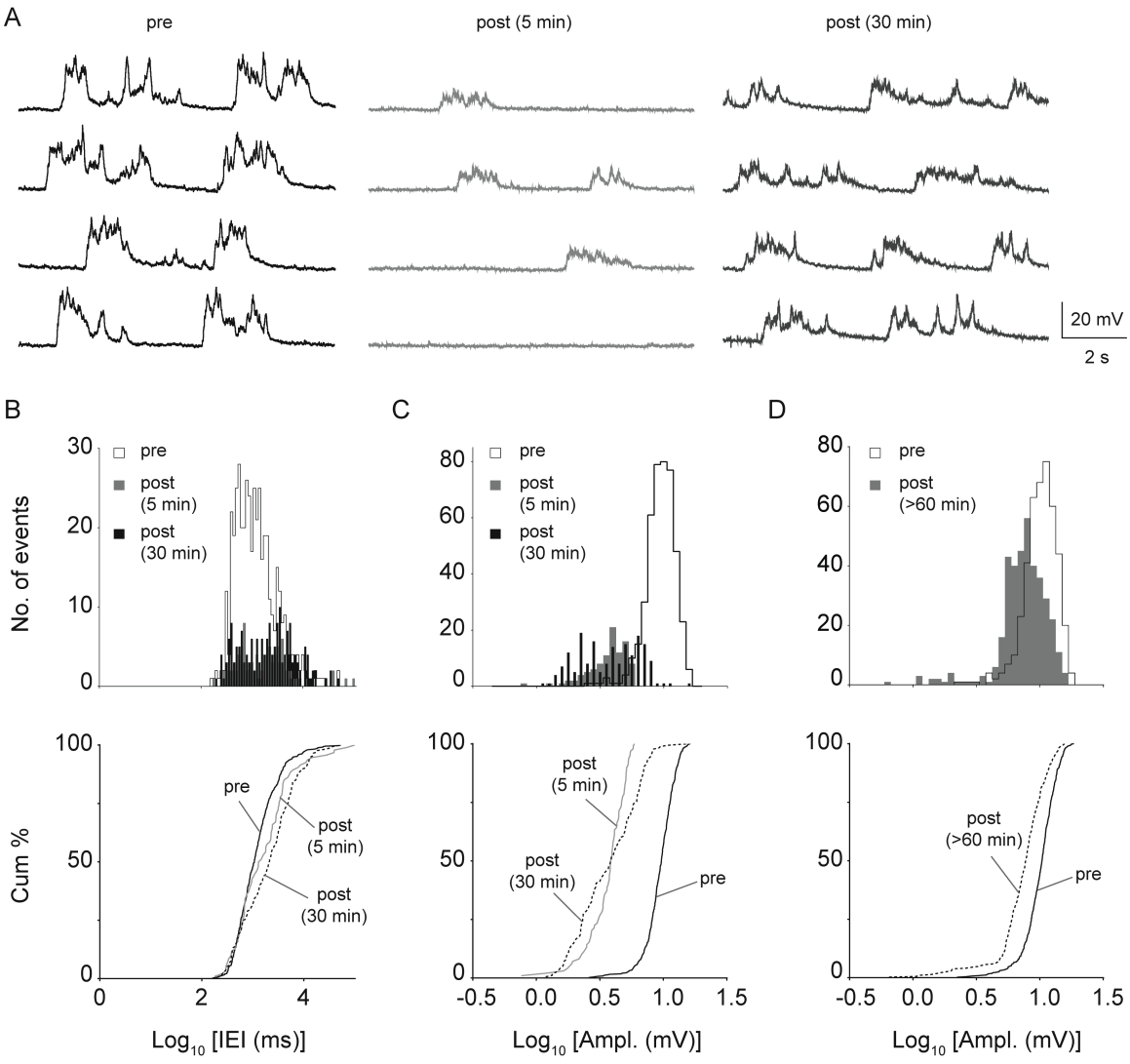

Supplementary Figure 4. Reduction in membrane up-states after CSD *in vivo*. (A) Representative traces of upstates are shown from layer 2/3 pyramidal neurons in pre-CSD and post-CSD groups. Slow oscillatory rhythms consisting of depolarized potential (upstates) and hyperpolarized state (downstates) were routinely observed before CSD. (B) Frequency of upstates is significantly decreased both 5 and 30 min after CSD (5 min: $p = 0.004$; 30 min: $p = 4.91*10^{-9}$; 2-sample KS test; n = 6 cells, 6 mice). (C) Amplitude of upstates is also reduced in both post-CSD groups (5 min: $p = 1.78*10^{-65}$; 30 min: $p = 6.18*10^{-71}$; KS test). (D) Upstate amplitude remained lower >60 min after CSD ($p = 1.34*10^{-28}$; KS

test). By this time upstate frequency had recovered ($p > 0.05$, KS test; data not shown). As upstates require recurrent network activity, these data are evidence that CSD affects network function beyond the local synapse.

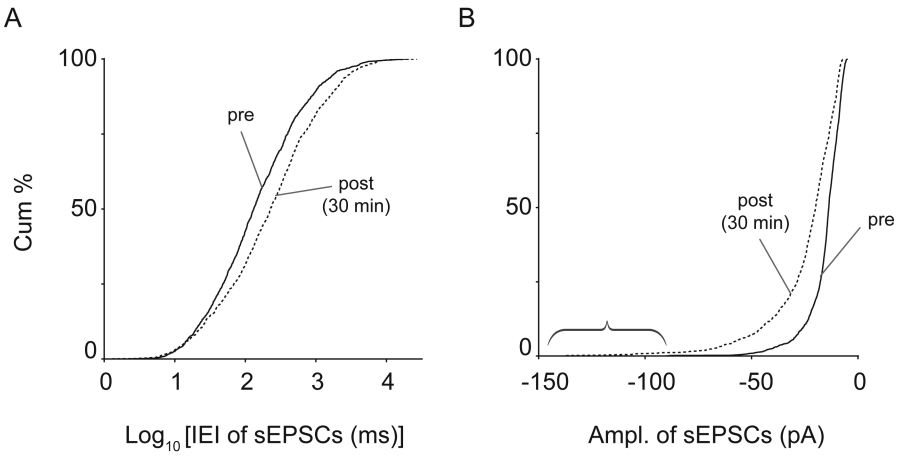

Supplementary Figure 5. Reduced frequency and increased amplitude of sEPSCs 30 min post-CSD *in vitro,* using potassium gluconate internal solution. Most *in vitro* recordings were performed in voltage clamp mode, using cesium-containing internal solution. However recordings in current clamp using potassium gluconate internal solution (identical to *in vivo* recordings) showed the same phenotype of decreased frequency (A) (KS test, $p = 3.53*10^{-13}$; n = 6 cells, 6 mice) and increased amplitude (B) of sEPSCs 30 min after CSD ($p = 1.42*10^{-85}$, KS test; bracket shows > 100 pA events).

References

Akerboom J, Chen TW, Wardill TJ, Tian L, Marvin JS, Mutlu S, Calderon NC, Esposti F, Borghuis BG, Sun XR, Gordus A, Orger MB, Portugues R, Engert F, Macklin JJ, Filosa A, Aggarwal A, Kerr RA, Takagi R, Kracun S, Shigetomi E, Khakh BS, Baier H, Lagnado L, Wang SS, Bargmann CI, Kimmel BE, Jayaraman V, Svoboda K, Kim DS, Schreiter ER, Looger LL. 2012. Optimization of a GCaMP calcium indicator for neural activity imaging. J Neurosci. 32:13819-13840.

Avermann M, Tomm C, Mateo C, Gerstner W, Petersen CC. 2012. Microcircuits of excitatory and inhibitory neurons in layer 2/3 of mouse barrel cortex. J Neurophysiol. 107:3116-3134.

Chung S, Li X, Nelson SB. 2002. Short-term depression at thalamocortical synapses contributes to rapid adaptation of cortical sensory responses in vivo. Neuron. 34:437-446.

Connors BW, Gutnick MJ. 1990. Intrinsic firing patterns of diverse neocortical neurons. Trends Neurosci. 13:99-104.

Connors BW, Gutnick MJ, Prince DA. 1982. Electrophysiological properties of neocortical neurons in vitro. J Neurophysiol. 48:1302-1320.

Ferster D, Jagadeesh B. 1992. EPSP-IPSP interactions in cat visual cortex studied with in vivo whole-cell patch recording. J Neurosci. 12:1262-1274.

Kawabata I, Kashiwagi Y, Obashi K, Ohkura M, Nakai J, Wynshaw-Boris A, Yanagawa Y, Okabe S. 2012. LIS1-dependent retrograde translocation of excitatory synapses in developing interneuron dendrites. Nat Commun. 3:722.

Kitamura K, Judkewitz B, Kano M, Denk W, Hausser M. 2008. Targeted patch-clamp recordings and single-cell electroporation of unlabeled neurons in vivo. Nat Methods. 5:61-67.

Margrie TW, Meyer AH, Caputi A, Monyer H, Hasan MT, Schaefer AT, Denk W, Brecht M. 2003. Targeted whole-cell recordings in the mammalian brain in vivo. Neuron. 39:911-918.

Markram H, Toledo-Rodriguez M, Wang Y, Gupta A, Silberberg G, Wu C. 2004. Interneurons of the neocortical inhibitory system. Nat Rev Neurosci. 5:793-807.

Mateo C, Avermann M, Gentet LJ, Zhang F, Deisseroth K, Petersen CC. 2011. In vivo optogenetic stimulation of neocortical excitatory neurons drives brain-state-dependent inhibition. Curr Biol. 21:1593-1602.

McCormick DA, Connors BW, Lighthall JW, Prince DA. 1985. Comparative electrophysiology of pyramidal and sparsely spiny stellate neurons of the neocortex. J Neurophysiol. 54:782-806.

Nowak LG, Azouz R, Sanchez-Vives MV, Gray CM, McCormick DA. 2003. Electrophysiological classes of cat primary visual cortical neurons in vivo as revealed by quantitative analyses. J Neurophysiol. 89:1541-1566.

Nunez A, Amzica F, Steriade M. 1993. Electrophysiology of cat association cortical cells in vivo: intrinsic properties and synaptic responses. J Neurophysiol. 70:418-430.

Sohya K, Kameyama K, Yanagawa Y, Obata K, Tsumoto T. 2007. GABAergic neurons are less selective to stimulus orientation than excitatory neurons in layer II/III of visual

cortex, as revealed by in vivo functional Ca2+ imaging in transgenic mice. J Neurosci. 27:2145-2149.

Tamamaki N, Yanagawa Y, Tomioka R, Miyazaki J, Obata K, Kaneko T. 2003. Green fluorescent protein expression and colocalization with calretinin, parvalbumin, and somatostatin in the GAD67-GFP knock-in mouse. J Comp Neurol. 467:60-79.

Tan AY, Brown BD, Scholl B, Mohanty D, Priebe NJ. 2011. Orientation selectivity of synaptic input to neurons in mouse and cat primary visual cortex. J Neurosci. 31:12339-12350.

Timofeev I, Grenier F, Steriade M. 2000. Impact of intrinsic properties and synaptic factors on the activity of neocortical networks in vivo. J Physiol Paris. 94:343-355.

Wang Z, McCormick DA. 1993. Control of firing mode of corticotectal and corticopontine layer V burst-generating neurons by norepinephrine, acetylcholine, and 1S,3R-ACPD. J Neurosci. 13:2199-2216.

Wilent WB, Contreras D. 2004. Synaptic responses to whisker deflections in rat barrel cortex as a function of cortical layer and stimulus intensity. J Neurosci. 24:3985-3998.

Zhu JJ, Connors BW. 1999. Intrinsic firing patterns and whisker-evoked synaptic responses of neurons in the rat barrel cortex. J Neurophysiol. 81:1171-1183.